Computing and Informatics, Vol. 44, 2025, 933–960, doi: 10.31577/cai_2025_4_933

AN AGGREGATION DEGREE-BASED COOPERATIVE MODEL FOR AUTONOMOUS VEHICLE GROUPS IN A CLOSING SCENE

Guiyuan Yuan

College of Computer Science and Engineering
Shandong University of Science and Technology
Qingdao 266590, China
e-mail: gyuan_yuan@163.com

Jiake Wang

University of Sydney
Camperdown, NSW 2050, Australia
e-mail: jwan0940@uni.sydney.edu.au

Fengqi Yan

Shanghai Heyeah IT Co., Ltd.
Shanghai 266426, China
e-mail: yanfengqi@heyeah.cn

Feng Shen

Shanghai Seari Intelligent System Co, Ltd.
Shanghai 200067, China
e-mail: shenfengtj@163.com

Xiangmei Li*, Jiujun Cheng

Key Laboratory of Embedded System and Service Computing
Ministry of Education, Tongji University, Shanghai 200092, China
e-mail: {lixiangmei, chengjj}@tongji.edu.cn

* Corresponding author

Abstract. Maintaining stable and orderly intelligent autonomous driving behavior in a closing scene is an important challenge. Compared with traditional chaos caused by an individual autonomous vehicle based on central control, when it breaks down, an intelligent cooperative autonomous driving group may effectively mitigate or alleviate the issue. There is no method to formulate an autonomous vehicle group and analyze its cooperative behavior by taking the aggregation, leading node change rate, and algorithm complexity of a vehicle group into account. This work formulates an aggregation degree-based Cooperative Model for Autonomous Vehicle Groups in a closing scene (CMAVG). First, we construct multi-roles and hierarchical autonomous vehicle groups. Then, we analyze their evolution behavior and present a dynamic evolution method based on it. Finally, we formulate CMAVG and give its solving method. We conduct extensive simulations in a simulated closing scene and a real one. Experimental results show that our autonomous vehicle group formation method outperforms a VANET clustering method and an autonomous vehicle group formation method in terms of aggregation degree, running time, and leading node change rate. CMAVG outperforms two cooperation methods for Internet of vehicles and an autonomous vehicle group cooperation method in terms of aggregation degree, leading node change rate, and vehicle group survival time.

Keywords: Autonomous vehicle group, closing scene, cooperative model, aggregation degree, multi-objective optimization

1 INTRODUCTION

Autonomous vehicle technology is developing rapidly with the breakthrough of artificial intelligence technology, which is expected to effectively alleviate traffic problems, e.g., congestion, accidents, and air pollution [1, 2]. Hence, it is of great interest to researchers and industries due to its capability of dynamically perceiving surrounding environments via multiple sensors. The perception combined with a vehicle's knowledge of dynamics and kinematics ensures safe travel on designed paths.

However, many challenges remain unresolved in the autonomous vehicle field. For example, once autonomous vehicles' perception fails, their driving system may collapse immediately and cause serious accidents. Static path planning methods cannot effectively address chaotic and disorderly movements caused by sudden system failures. Additionally, unpredictable road environments, complex interactions between vehicles, and limitations in current sensor technology introduce significant challenges in ensuring the robustness and adaptability of autonomous systems. There is a need for advanced methods to handle edge cases, such as sensor blind spots, adverse weather conditions, and unexpected dynamic obstacles, which remain difficult to model and predict accurately.

Compared with a single vehicle, an autonomous vehicle group has a larger perception range via internal communications, which can avoid potential risks caused by blind spots. However, challenges arise in maintaining stable and reliable commu-

nications within and between vehicle groups, particularly in dynamic environments with high vehicular density or potential signal interference. Establishing a stable and orderly autonomous vehicle group capable of cooperation is essential to ensure all vehicles maintain intelligent and safe autonomous driving behavior. This requires addressing problems such as group coordination under varying traffic conditions, scalability of communication protocols, and adaptive decision-making mechanisms that can respond to rapidly changing group configurations. There are many studies [3, 4, 5, 6, 7, 8] focusing on information dissemination among vehicles, although none of them apply effectively to cooperative interactions within an autonomous vehicle group. Furthermore, existing work often overlooks the impact of environmental and operational constraints, such as varying road infrastructures, bandwidth limitations, and efficiency of communication modules, on the design of cooperative models.

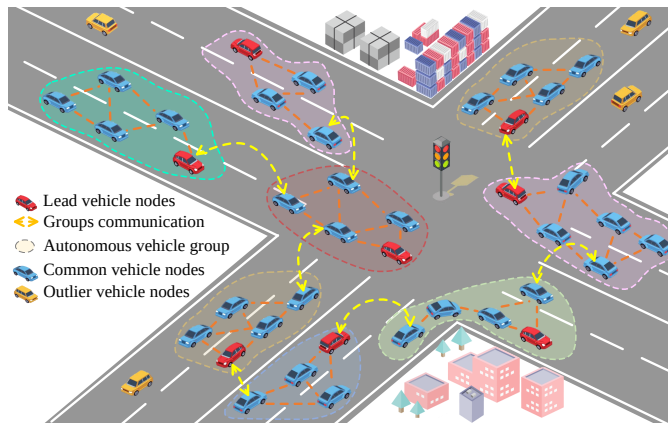

Figure 1. Autonomous vehicle groups in a closing scene

Existing studies mainly focus on autonomous vehicle group formation [9, 10, 11, 12, 13, 14, 15, 16] and dynamic evolution [17, 18, 19, 20, 21, 22, 23, 24, 25], but they suffer from low network connectivity, poor real-time performance, and limited scalability in complex scenarios. Moreover, few methods address how to achieve optimal balance among multiple objectives under conflicting constraints. Closing scene is a scene without external disturbances, e.g., pedestrians, obstacles, and manned vehicles. Each vehicle belongs to a group that is guided by a leading vehicle. The connection among vehicle groups depends on vehicles within the perception range of each other. As shown in Figure 1. First, we study vehicle states in an autonomous vehicle group and propose an Autonomous Vehicle Group Model (AVGM) based on node joining, node leaving, and leading node replacement strategies. Then, we study the dynamic evolution behavior of autonomous vehicle groups and formulate an aggregation degree-based Cooperative Model for Autonomous Vehicle Groups (CMAVG) in a closing scene by using finite state machine theory. Finally, we pro-

pose a multi-objective optimization method to solve CMAVG. Our contributions are:

1. To form a hierarchical multi-role autonomous vehicle group, we define four autonomous vehicle roles, i.e., initialize, leading, common, and outlier. Then, we formulate an autonomous vehicle group model based on aggregation degree to ensure its stability;
2. To analyze the dynamic evolution behavior of autonomous vehicle groups, we define five dynamic evolution events, i.e., initialization, joining, leaving, leading node selection, and leading node replacement. Based on which we formulate six dynamic evolution statuses and a state transition process by using a finite state machine theory;
3. To maintain cooperative behavior among group members, we propose a collaborative model for autonomous vehicle groups, formulate CMAVG, and introduce a multi-objective optimization method to solve it; and
4. To verify the effectiveness of the proposed autonomous vehicle group formation and cooperative method, we construct a simulated closing scene and a real one and conduct extensive simulations in two scenes to demonstrate the performance of our method in terms of aggregation degree, running time, leading node change rate, and vehicle group survival time.

The rest of this paper is organized as follows. Section 2 introduces related work. Section 3 presents an autonomous vehicle group model. Section 4 introduces a cooperative model for vehicle groups. Section 5 shows the experimental results in simulated and real scenes. Section 6 concludes this work.

2 RELATED WORK

2.1 Vehicle Group Formation

Jalil et al. [9] divide vehicles that are entering an island into vehicle groups. The authors propose a vehicle speed-adjusting method to improve traffic efficiency. However, their method faces high time complexity when the number of vehicles is large. Bakibillah et al. [10] propose a bi-level control system for autonomous vehicles at roundabouts. They divide island areas into a formation area and a merging one, merge some adjacent vehicle groups, and adjust the speed of vehicle group members. However, it is difficult to achieve real-time speed optimization on a high-traffic island. Chang and Ning [11] construct vehicle groups by using an improved K-means algorithm. However, its performance decreases as the vehicle mobility capacity increases. Wang et al. [12] construct vehicle groups based on autonomous vehicles' lane information, based on which they design four control patterns, i.e., acceleration, deceleration, maintenance, and emergency. However, the computational complexity of these patterns increases with the number of vehicles. Ghiasi et al. [13] use leading vehicles to control vehicle group members by using the information gathered

by sensors and other autonomous vehicles. Their method shows good performance in a mixed-traffic environment where human-driven and autonomous vehicles coexist. Yu et al. [14] use graphs to model dependencies among autonomous vehicles and introduce a reinforcement learning-based mobility adjusting method for their members. However, their method suffers from low convergence when the traffic environment is highly dynamic. Nakamura and Sakakibara [15] introduce a verification method for autonomous vehicle group control, which uses a temporal automaton to model their dynamic behavior. Nevertheless, their method only considers a resource-intensive scene, which is not suitable for a real mixed-traffic environment. Maiti et al. [16] compare a greedy strategy-based vehicle group formation method with a destination-based one. Their studies highlight the trade-offs between vehicle group formation speed and fuel efficiency.

2.2 Dynamic Evolution

Dokur et al. [17] control the relative angle of autonomous vehicles to form vehicle groups. Although their method ensures smooth integration of a vehicle into a vehicle group by managing its orientation, it is difficult to precisely control a vehicle's angle in a real scene. El Ganaoui-Mourlan et al. [18] generate paths of vehicle group members based on model prediction control and fast search random tree, which can ensure smooth vehicle group formation. Yet, their model prediction control method has a high computational requirement. Sreenivasamurthy and Obraczka [19] compare the mobility behavior of vehicle group members as behavior in biological systems, based on which they design joining and leaving strategies. However, this decentralized vehicle group structure leads to unstable of following relationship among vehicle group members. Wu et al. [20] use reliable attribute encryption and blockchain to revoke the secret keys of malicious nodes in autonomous vehicle groups. Xiong et al. [21] use a Markov decision-making process to decide whether an autonomous vehicle entering a highway can join a vehicle group. However, Markov decision-making processes suffer from high computational expenses. Ge et al. [22] introduce mobility strategies for vehicle group members in merging and splitting events. Their strategies use resilient control mechanisms to handle uncertainties, its complexity is high when there are several vehicle groups interacting with each other. Ye et al. [23] introduce mobility strategies for autonomous vehicle groups in merging and lane-changing events. Their method ensures autonomous vehicles adjust their speed in a multi-lane highway, which assumes that other vehicles follow mobility patterns. Kato et al. [24] divide autonomous vehicles near a ramp into vehicle groups, where a leading vehicle determines the time entering a main road. However, a leading vehicle may make error decisions in a real scene. Zhou and Zhu [25] analyze the effects of vehicle group size on its evolutionary behavior. Nevertheless, their analysis is a theoretical model, which does not consider the real-world factors such as communication delays, sensor errors, and unexpected traffic disruptions.

2.3 Summary

In recent years, research on autonomous vehicle groups has attracted attention from academia and industry. Most existing studies do not consider the safe driving behavior issues caused by the possible evolution of vehicle groups in an unstable state. Therefore, it is critical to establish a vehicle group model, study its dynamic evolution, and propose a cooperative model to maintain a stable and orderly intelligent autonomous driving behavior.

3 AUTONOMOUS VEHICLES GROUP MODEL

In this section, we formulate an autonomous vehicle group model. First, we give some formal definitions. Then, we introduce four autonomous vehicle states. Next, we define three performance metrics for autonomous vehicle groups. Finally, we present the autonomous vehicle group model based on a vehicle group actions.

3.1 Formal Specification

Autonomous vehicles communicate with each other, based on which they collect the neighbor autonomous vehicle information and construct autonomous vehicle groups. Hence, we define the formal definition of autonomous vehicle connect factor, neighbor node set, vehicle node leading degree, and vehicle connectivity cost.

Definition 1. The autonomous vehicle connect factor $C_t(v_a, v_b)$ between vehicles v_a and v_b at time t is

$$C_t(v_a, v_b) = \begin{cases} 1, & d_t(v_a, v_b) \leq R, \\ 0, & \text{otherwise}, \end{cases} \tag{1}$$

where $d_t(v_a, v_b)$ denotes the distance between v_a and v_b at t and R denotes the communication range of autonomous vehicles.

Definition 2. The neighbor node set $K_t(a)$ of v_a at t is

$$K_t(v_a) = \{v_b | (C_t(v_a, v_b) > 0) \wedge (v_b \notin \{\emptyset, v_a\}), v_a, v_b \in S\}, \tag{2}$$

where S denotes a vehicle set.

Definition 3. The vehicle node leading degree $L_t(v)$ of vehicle v at t is

$$L_t(v) = \sqrt{l_t(v, x) + l_t(v, y)}, \tag{3}$$

where $l_t(v, x)$ and $l_t(v, y)$ represent the leading degree in the direction of x and y of coordinate axes, respectively, i.e.,

$$l_t(v, o) = (h_t(v, o) + \alpha s_t(v, o) - \frac{\sum_{v_j \in G_t(v)} h_t(v_j, o)}{|G_t(v)|})^2, \tag{4}$$

where $l_t(v, o)$ represents the leading degree of vehicle v in direction o, $h_t(v, o)$ represents the coordinate of v in direction o at t, $s_t(v, o)$ represents travel speed of v in direction o, α represents a weight, $G_t(v)$ represents a vehicle group where node v is located at t, and $|G_t(v)|$ represents the corresponding number of vehicles.

Definition 4. Vehicle connectivity cost $\tilde{C}_t(v_a)$ of vehicle v_a within its communication range is

$$\tilde{C}_t(v_a) = \sum_{\substack{v_b \in G_t(v_a) \\ w_{a,b} \in A_c}} w_{a,b} C_t\left(v_a, v_b\right), \tag{5}$$

where A_c is an adjacency matrix of connection weights and $w_{a,b}$ represents connection weight between v_a and v_b.

3.2 Autonomous Vehicle States

To describe the formation process of autonomous vehicle groups, we define the following four autonomous vehicle states.

3.2.1 Leading State

An autonomous vehicle group only has one leading node. To ensure structural stability of a vehicle group, a leading node has the highest leading degree within a vehicle group, i.e.,

$$\mathcal{L}_t = \underset{v \in G_t}{\operatorname{argmax}}\ L_t(v), \tag{6}$$

where $\mathcal{L}_t$ represents a leading node in a vehicle group G at t.

3.2.2 Common State

Except for a leading node, the remaining group members are in a common state in a vehicle group. If a vehicle group loses a leading node, a common node changes into a new leading node through competition, a vehicle v is in common state if

$$(v \in G) \wedge (\exists \hat{v} \Rightarrow (L_t(v) < L_t(\hat{v}))). \tag{7}$$

3.2.3 Initialize State

Initialize state is an initial state of an autonomous vehicle. If an autonomous vehicle is in an initialize state, it needs to collect neighbor vehicle information. A vehicle v is in initialize state if

$$(\forall G \Rightarrow v \notin G) \wedge (L_t(\hat{v}) = 0). \tag{8}$$

3.2.4 Outlier State

An autonomous vehicle in an outlier state if it does not belong to a vehicle group and all vehicle group members near it refuse to join, i.e.,

$$(\forall G \Rightarrow v \notin G) \wedge (L_t(\hat{v}) \geq 0). \tag{9}$$

3.3 Performance Metrics

To evaluate the performance of autonomous vehicle groups, we introduce the following three metrics.

3.3.1 Aggregation Degree

The aggregation degree $a(v_i)$ measures the cohesion and separation of vehicle group division results. It includes

$$a(v_i) = \frac{k(v_i) - m(v_i)}{k(v_i) + m(v_i)}, \tag{10}$$

$$k(v_i) = \frac{\sum_{v_i, v_j \in G} d(v_i, v_j)}{|G|}, \tag{11}$$

$$r(v_i) = \frac{\sum_{v_i \in S} \sum_{v_j \in S \setminus G(v_i)} \tilde{d}(v_i, v_j)}{|\widetilde{G}|}, \tag{12}$$

where $k(v_i)$ denotes similarity within a vehicle group, which is the average distance from vehicle v_i to vehicle v_j in a vehicle group, $r(v_i)$ represents the difference degree outside a vehicle group, which is the average distance between v_i and v_j with the same destination outside a vehicle group, $\tilde{d}(v_i, v_j)$ represents the distance between v_i and v_j with the same destination, $|\widetilde{G}|$ denotes the number of vehicle groups.

From the definition of aggregation degree, larger aggregation degree indicates higher closeness of a vehicle group.

3.3.2 Algorithm Running Time

The running time of an algorithm starts from the time of all autonomous vehicles in an initial state to the time of all vehicles in an orderly state, i.e.,

$$T = \sum_{G_i \in \widetilde{G}} T^* (G_i) - T^0 (G_i), \tag{13}$$

where $\widetilde{G}$ represents a vehicle group set, $T^*(G_i)$ denotes the time at which vehicle group G_i is stabilized, and $T^0 (G_i)$ denotes the time at which vehicle group G_i is in an initial state.

3.3.3 Leading Node Change Ratio

The leading node change ratio I represents the ratio of leading node change count with respect to the number of vehicle group members, i.e.,

$$I = \frac{I_t(G)}{|G_t|}, \tag{14}$$

where $I_t(G)$ represents the number of leading node changes in vehicle group G at t.

3.4 Autonomous Vehicle Group Model

An autonomous vehicle group is a hierarchical multi-role structure. Hence, its model is

$$M = (S, B, W, \widetilde{G}, \widetilde{\mathcal{L}}, \widetilde{V}, \widetilde{O}, F), \tag{15}$$

where $\widetilde{G} = \{G_i = (\widetilde{\mathcal{L}}_i, \widetilde{V}_i) \mid i = 1, 2, 3, \ldots, n\}$ represents a vehicle group set, $\widetilde{\mathcal{L}}$ denotes a leading node set, $\widetilde{V}$ denotes a common node set, $\widetilde{O}$ is an outlier node set, $F = \{f_i \mid i = 1, \ldots, k\}$ is a function set for vehicle group node actions. Our vehicle group model has the following four actions.

3.4.1 Initialization f_1

All vehicle nodes are initialized into common nodes $\widetilde{V} = \{v_i \mid \forall v_i \in S\}$. Then a leading node is selected by traversing $\widetilde{V}$. The following two steps are executed iteratively.

1. Selecting a node $v_i \in \widetilde{V}$ and adding it to leading node set $\widetilde{\mathcal{L}} = v_i \cup \widetilde{\mathcal{L}}$; and
2. Updating vehicle group G_i containing leading node v_i by $G_i = (v_i, \{v_j \mid (D(v_j) = D(v_i)) \wedge (A(v_i, v_b) = 1), \forall v_j \in \widetilde{V}\})$ and updating a common node set by $\widetilde{V} = \widetilde{V} \backslash G(v_i)$, where $D(v)$ indicates v's destination.

   Repeating the above process until $\widetilde{V}$ is empty.

3.4.2 Joining f_2

If there exists $v_j \in \widetilde{O}$, v_j joins a suitable vehicle group G_i within its communication range. Updating $G_i^{'}$s information $\widetilde{V}_i = v_j \cup \widetilde{V}_i$ and $\widetilde{O} = \widetilde{O} \backslash v_j$. A leading node decides whether a joining request is passed through a decision function, which takes the vehicle group size, connectivity cost, and connectivity strength into account, i.e.,

$$\text{decision}(\Delta H, \Delta V, |G|, \tilde{C}) = \frac{m\tilde{C} + n|G|}{1 + e^{-(\sqrt{\Delta H + \Delta V} - \eta)}},$$

where ΔH and ΔV represent the position difference and velocity difference, respectively, η is an adjustment parameter, and $|G|$ denotes the number of vehicles in vehicle group G.

A leading node permits a joining request if its decision function value is less than threshold α.

3.4.3 Leaving f_3

Vehicle group members sense neighboring vehicles by periodically receiving data packets broadcasted from them. All vehicles maintain an adjacency information table and decide whether adjacent vehicles leave a vehicle group by receiving data within a given amount of time t^*. If v_j does not send data to its neighboring vehicles within t^*, neighboring nodes send a message packet to leading node v_i to report that a vehicle has left. A leading node updates G_i's information $G_i = (v_i, \widetilde{V}_i \backslash v_j)$.

3.4.4 Leading Node Selection and Replacement f_4

A leading node is at the front of a vehicle group. The node with the highest leading degree value is selected as a new leading node through a broadcast mechanism when a leading node updates its leading degree value. If their destination is different, different vehicle groups are formed, and the vehicles with different destinations are automatically selected as leading nodes. Therefore, if $\mathcal{L}_i$ is empty, then G_i selects a new leading node $v_j = \underset{v \in \widetilde{V}_i}{arg\max}\, L(v)$ and then removes it from $\widetilde{V}_i$. The vehicle group is represented as $G_i = (v_j, \widetilde{V}_i \backslash v_j)$.

4 COOPERATIVE MODEL FOR AUTONOMOUS VEHICLE GROUPS

In this section, we first propose a dynamic evolution method. Then, we formulate CMAVG. Finally, we present a multi-objective optimization method to solve CMAVG.

4.1 Autonomous Vehicle Representation

To describe mobility attributes of autonomous vehicle groups, we give autonomous vehicle representation E_t, i.e.,

$$E_t = \{G_t, V_t, D_t, P_t, O_t\}, \tag{16}$$

where G_t is an autonomous vehicle group, V_t is vehicle velocity, D_t is vehicle driving direction within the range of 0° and 360°, $P_t = (x_t, y_t)$ is a two-dimensional coordinate vector, and $O_t = (o_x, o_y)$ is vehicle destination.

The vehicle similarity $S(v_a(t), v_b(t))$ between autonomous vehicles v_a and v_b is

$$S(v_a(t), v_b(t)) = \begin{cases} \|E_t(v_a) - E_t(v_b)\|_2, & \text{if } k \le \|E_t(v_a) - E_t(v_b)\|_2, \\ 0, & \text{otherwise}, \end{cases} \tag{17}$$

where k is a threshold to judge whether a vehicle group is cooperating.

4.2 CMAVG

CMAVG considers two parts: intra-group and inter-group. We exploit the relevant knowledge of autonomous vehicle group evolution algorithms based on finite state machine theory. Each vehicle group can be regarded as a sub-model of a cooperative model and each sub-model has a merge algorithm to fuse other sub-models into a cooperation model. Each sub-model is composed of four tuples, i.e.,

$$\mathcal{S} = (\mathcal{Z}, \mathcal{U}, \delta, \mathcal{Q}, \mathcal{F}), \tag{18}$$

where $\mathcal{Z}$ is a state set, $\mathcal{U}$ is an input set, δ is a mapping from $\mathcal{U}$ to $\mathcal{Z}$, $\mathcal{Q}$ is a non-empty initial state, and $\mathcal{F}$ is a terminal state set.

The state transition of a cooperation model within a vehicle group is shown in Figure 2. Next, we introduce the definition of each state:

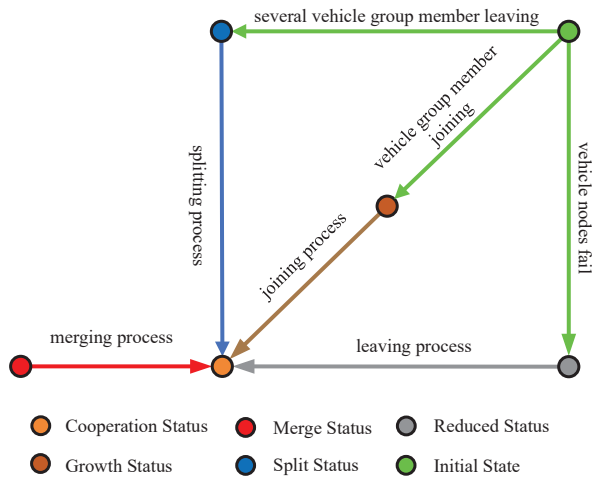

Figure 2. State transition of a vehicle group

4.2.1 Initial Status $\mathcal{Z}_1$

In an initial state, a vehicle group can maintain status and move stably and its members and leading nodes remain unchanged, i.e.,

$$\widetilde{S}_G(t, t+1) < 0.5, \tag{19}$$

where $\widetilde{S}_G$ calculates the similarity of vehicle group G from t to $t+1$.

4.2.2 Growth Status $\mathcal{Z}_2$

In a growth status, existing vehicles request to join a vehicle group G through a vehicle group evolution algorithm, i.e.,

$$\widetilde{D}_G(t, t+1) > 0, \tag{20}$$

where $\widetilde{D}_G$ calculates the difference of vehicle group member count from t to $t+1$.

4.2.3 Reduced Status $\mathcal{Z}_3$

In a reduced status, existing vehicles may lose contact with a vehicle group due to emergency events. Hence, its size is reduced, i.e.,

$$\widetilde{D}_G(t, t+1) < 0. \tag{21}$$

4.2.4 Split Status $\mathcal{Z}_4$

A vehicle group is in a split status when some vehicle group members lose communications with others because of an intersection or traffic lights, i.e.,

$$\widetilde{D}_G(t, t+1) < 0, \tag{22}$$

$$\widetilde{N}_G(t, t+1) > 1, \tag{23}$$

where $\widetilde{N}_G$ calculates the change of the number of vehicle groups.

4.2.5 Merge Status $\mathcal{Z}_5$

Different from a split status, a merge state denotes that two vehicle groups are merged into a new vehicle group when they are close to each other, i.e.,

$$\widetilde{D}_G(t, t+1 align > 0, \tag{24}$$

$$\widetilde{N}_G(t, t+1) < 1. \tag{25}$$

4.2.6 Cooperation Status $\mathcal{Z}_6$

Cooperation status indicates that the typology of a vehicle group remains unchanged within a period, i.e.,

$$\tilde{T} = \sum_{v_a, v_b \in G} \tilde{M}(v_a, v_b), \tag{26}$$

$$\widetilde{S}_G(t, t+1) = 1, \tag{27}$$

where $\widetilde{T}$ calculates the connectivity cost between v_a and v_b in G.

When the average value of S between two moments is greater than 0.5, it means that a vehicle group is cooperative.

4.3 Multi-Objective Optimization for CMAVG

4.3.1 Objective Function

Our cooperative model can be divided into two parts: A model within a vehicle group and a model among vehicle groups. The former is expressed as $\mathcal{S}_i = (\mathcal{Z}_i, \mathcal{U}_i, \delta_i, \mathcal{Q}_i, \mathcal{F}_i)$, and the latter is expressed as:

$$\hat{\mathcal{S}} = \omega_1 \mathcal{S}_1 + \omega_2 \mathcal{S}_2 + \cdots + \omega_n \mathcal{S}_n, \tag{28}$$

where ω_i represents a weight of vehicle groups in a cooperative model.

CMAVG's goal is stability, real-time interactivity, and evolution of a vehicle group, i.e.,

$$F_1(G) = \sum_{v_i, v_j \in G} \rho_{i,j}, \tag{29}$$

$$F_2(G) = \max\left(\frac{d(v_i, v_l)}{\epsilon}\right), \quad v_i \in G, \tag{30}$$

$$F_3(G) = \sum_{v_i \in G} \Gamma_G(t, t+1), \tag{31}$$

where v_i and v_j are two vehicle group members in G, $\rho_{i,j}$ represents the edge weight between v_i and v_j, v_l is a leading node, ϵ is message propagation rate, and $\Gamma_G(t, t+1)$ is the number of vehicle group's evolutions from t to $t+1$.

4.3.2 Constraint Condition

For a cooperative model $\hat{\mathcal{S}}$, its parameter constraints are

$$(0 \leq \omega_i \leq 1) \wedge (1 \leq i \leq N). \tag{32}$$

The second constraint is the limit of vehicle group size, i.e.,

$$0 \leq N \leq N_v. \tag{33}$$

The connectivity between common nodes and a leading node in a vehicle group is

$$0 \leq F_1(G) \leq N. \tag{34}$$

4.3.3 Optimal Solution

According to an objective function and constraint conditions, CMAVG is

$$F(G_t) = \min[-F_1(G_t), F_2(G_t), F_3(G_t)], \tag{35}$$

$$\text{s.t.} \quad \begin{cases} 0 \le \omega_i \le 1, 1 \le i \le N, \\ 0 \le N \le |S|, \\ 0 \le F_1(G_t) \le N. \end{cases} \tag{36}$$

Considering that our cooperative model is composed of three objectives, we improve a simulated annealing algorithm to solve it. As shown in Algorithm 1, it inputs initial coefficient T_0, terminal coefficient T_f, judge coefficient ϵ_{th}, learning rate r, initial solution x, and vehicle counts N. First, it initializes coefficient T, iteration steps s, and solution x_s at step s (lines 2–4). Then, it randomly selects some vehicles to update solution x_s based on ϵ_{th} (lines 5–11). Next, it calculates the difference value of our cooperation model with solutions x_s and x_{s-1} and selects this solution if the difference value is greater than zero or with a probability (lines 12–21). Finally, it updates the coefficient T (line 22).

According to [26], initial coefficient determines the search width of Algorithm 1. Larger initial coefficient indicates longer convergence time. The terminal coefficient determines the search depth of Algorithm 1. Smaller terminal coefficient indicates higher computational complexity. The judge coefficient determines the acceptability of new solutions. Higher judge coefficient indicates higher acceptability of new solutions. The initial solution indicates the first solution of Algorithm 1. Higher similarity between an initial solution and an optimal one indicates lower convergence time, but the optimal solutions is difficult to calculate. Hence, we set the initial coefficient to 100, terminal coefficient to 0.01, judge coefficient to 0.99, and initial solution to $\{0, 0, \ldots, 0\}$.

Theorem 1. The time complexity of Algorithm 1 is

$$O_t = \log_r(T_f - T_0) * N, \tag{37}$$

where r is learning rate, T_f and T_0 are terminal coefficient and initial coefficient, respectively, and N is vehicle counts.

Proof. Algorithm 1 consists of two subprocesses, i.e., decrease of coefficient T_0 and solution x_s construction. In each coefficient decrease process, coefficient T decreases into $T \times r$, hence, the time complexity of decrease of coefficient T_0 is

$$O_t^1 = \log_r(T_f - T_0). \tag{38}$$

Algorithm 1 Multi-objective optimization method for CMAVG

Input: $F(G_t)$, initial coefficient T_0, terminal coefficient T_f, judge coefficient ϵ_{th}, learning rate r, initial solution $x = \{0, 0, 0, \dots\}$, and vehicle counts N.
$T = T_0$;
$s = 0$;
$x_s = x$;
while $T > T_f$ **do**
  $s = s + 1$;
  for $i < N$ **do**
    if $(\text{random}(0, 1) \leq \epsilon_{th}) \wedge (x_s[i] = 0)$ **then**
      $x_s[i] = 1$;
    end if
  end for
  Calculating $\Delta F(G_t) = F_{x_s}(G_t) - F_{x_{s-1}}(G_t)$;
  if $\Delta F(G_t) > 0$ **then**
    continue;
  else
    if $exp(\Delta F(G_t)) > \text{random}(0, 1)$ **then**
      continue;
    else
      $x_s = x_{s-1}$;
    end if
  end if
  $T = T \times r$;
end while
Output: CMAVG's solution x;

In each coefficient decrease process, Algorithm 1 construction solution x by randomly selecting candidate group members. Hence, its time complexity is

$$O_t^2 = N. \tag{39}$$

Hence, the time complexity of Algorithm 1 is

$$O_t = O_t^1 \times O_t^2 = \log_r(T_f - T_0) * N. \tag{40}$$

□

5 EXPERIMENT AND EVALUATION

5.1 Simulation Setting

In this section, we introduce simulation scenes, benchmark methods, and evaluation metrics in detail.

5.1.1 Simulation Scenes

In simulations, we construct a simulated closing scene and a real one by using Simulation of Urban MObility (SUMO) [27] and Open Street Map (OSM) [28], respectively. Their details are as follows:

1. A simulated closing scene: As shown in Figure 3, we use SUMO to construct a 10 km × 5 km closing scene without disturbances. There are 50 roads and 300 crossroads. Each crossroad has a traffic light. The detailed simulation parameters are shown in Table 1.

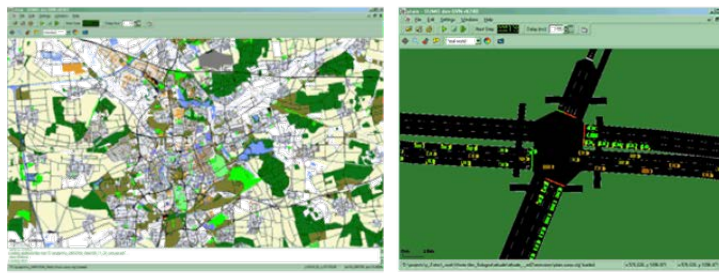

Figure 3. A simulated closing scene

Parameters	Values
Section size	10 km×5 km
Experiment time	20 minutes
Number of roads	50
Number of crossroads	300
Traffic light	yes
Traffic light time (red, yellow, green)	40 s, 3 s, 100 s
Vehicle counts	600
Communication range	150 m
Data packet size	32 Byte
Data receiving frequency	100 Hz

Table 1. Simulation parameters in a simulated closing scene

2. A real closing scene: We use OSM to construct a 6.5 km × 5.8 km real closing scene without disturbances. Its road typology is shown in Figure 4, which has 2 357 roads and 259 crossroads. The detailed simulation parameters are shown in Table 2.

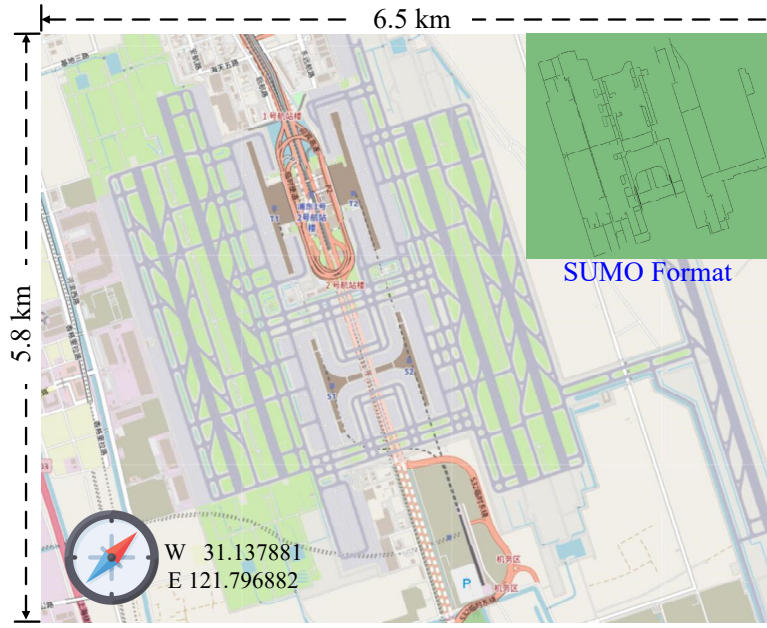

Figure 4. A real closing scene

5.1.2 Benchmark Methods and Evaluation Metrics

To verify the performance of our AVGM, we compare it with the performance of SOC [29] and AVGC [30]. We select SOC because it is one of the most famous clustering method for VANET that has been proposed in recent years and it demon-

Parameters	Values
Section size	6.5 km × 5.8 km
Experiment time	20 minutes
Number of roads	2 357
Number of crossroads	259
Traffic light	yes
Traffic light time (red, yellow, green)	40 s, 3 s, 100 s
Vehicle counts	600
Communication range	150 m
Data packet size	32 Byte
Data receiving frequency	100 Hz

Table 2. Simulation parameters for a real closing scene

strates better performance than a vehicle oriented clustering method [31]. We select AVGC because it is the latest autonomous vehicle group formation method that is published in a high impact factor journal. We use the following three metrics to measure the performance of AVGM, SOC, and AVGC:

1. Aggregation degree: It measures the closeness degree of a vehicle group. Higher aggregation degree indicates higher closeness among group members;
2. Running time: It measures the time duration of a vehicle group from an initial state to a stable one. Smaller running time indicates higher convergence efficiency; and
3. Leading node change rate: It measures the frequency at which a leading node within a vehicle group changes. Smaller leading node change rate indicates higher stability of a leading node.

To verify the effectiveness of the proposed CMAVG, we compare its performance with that of AVGC [30], Tracking Evolving Communities for Internet of vehicles (TEC) [27], and Passive Clustering-based Techniques (PCT) for Internet of vehicles [32]. We select AVGC because it is the latest autonomous vehicle group cooperation method published in a high impact factor journal. We select TEC and PCT because they are two typical cooperation methods for complex communities. In addition to aggregation degree and leading node change rate, we use vehicle group survival time to measure the performance of AVGM, SOC, and AVGC:

Vehicle group survival time: It measures the duration of a vehicle group from formation to disappearing. Higher vehicle group survival time indicates higher stability of a vehicle group.

5.2 Simulation Results in a Simulated Scene

5.2.1 Performance of Vehicle Group Model in a Simulated Closing Scene

The relationship between aggregation degree and vehicle speed of AVGM, SOC, and AVGC with different α values is shown in Figures 5 a), 5 b), 5 c). The aggregation degree of AVGM is higher than that of SOC and AVGC at different vehicle speed and α values, which verifies the effectiveness of our method. The aggregation degree decreases as vehicle speed increases for a fixed α because the vehicle speed difference among vehicle group members increases with their speed. The aggregation degree decreases as α increases because the number of vehicle group members increases with α, resulting in the increase of mobility difference among vehicle group members.

The relationship between running time and vehicle speed of AVGM, SOC, and AVGC with different α values is shown in Figures 5 d), 5 e), 5 f). AVGM's running time is shorter than SOC's and AVGC's, which verify the convergence of our method. The running time slightly increases with vehicle speed for a fixed α because the

vehicle density decreases as vehicle speed increases and vehicle group formation methods need a longer time to convergence.

The relationship between leading node change rate and vehicle speed of AVGM, SOC, and AVGC with different α values is shown in Figures 5 g), 5 h), 5 i). AVGM's leading node change rate is lower than SOC's and AVGC's because the mobility difference among group members increases with their speed, which results in frequent changing of leading nodes and association relationship among group members. AVGM's leading node change rate increases with α because the vehicle group size increases with α, which leads to the increase of mobility difference between a leading node and its following nodes.

From Figure 5, AVGM's aggregation degree is higher than SOC's and AVGC's and its running time and leading node change rate is lower than SOC's and AVGC's at different vehicle speed and α values, which verifies AVGM's effectiveness in a simulated closing scene.

5.2.2 Performance of Cooperative Model in a Simulated Closing Scene

As shown in Figures 6 a), 6 b), 6 c), 6 d), we show the aggregation degree of four cooperation methods for a small time scale and the entire simulated process, respectively. CMAVG shows the best performance for a small time scale and the entire simulated process. The aggregation degree of CMAVG, AVGC, TEC, and PCT increases with time and is stable after 0.5 s. Compared Figure 6 b) with Figure 6 a), we observe that the aggregation degree of AVGC, TEC, and PCT increases after multi-objective optimization is used. This is because our multi-objective optimization method optimizes vehicle group structures.

As shown in Figures 6 e), 6 f), we show the changing process of leading node change rate of CMAVG, AVGC, TEC, and PCT. Each point represents the average existence time of a vehicle group within 10 minutes. Experimental results show that CMAVG obtains the best performance and the leading node changing rate of AVGC, TEC, and PCT decrease after optimizing a cooperative model.

As shown in Figures 6 g), 6 h), we show the changing process of vehicle group survival time of CMAVG, AVGC, TEC, and PCT. CMAVG's vehicle group survival time is longer than AVGC's, TEC's, and PCT's. After using a multi-objective optimization method, AVGC's vehicle group survival time is increased by 2.5 s, TEC's vehicle group survival time is increased by 3 s, and PCT's vehicle group survival time is increased by 5 s, which verifies the effectiveness of our multi-objective optimization method.

5.3 Simulation Results in a Real Closing Scene

5.3.1 Performance of Vehicle Group Model in a Real Closing Scene

The relationship between aggregation degree and vehicle speed of AVGM, SOC, and AVGC with different α values is shown in Figure 7. The aggregation degree decreases

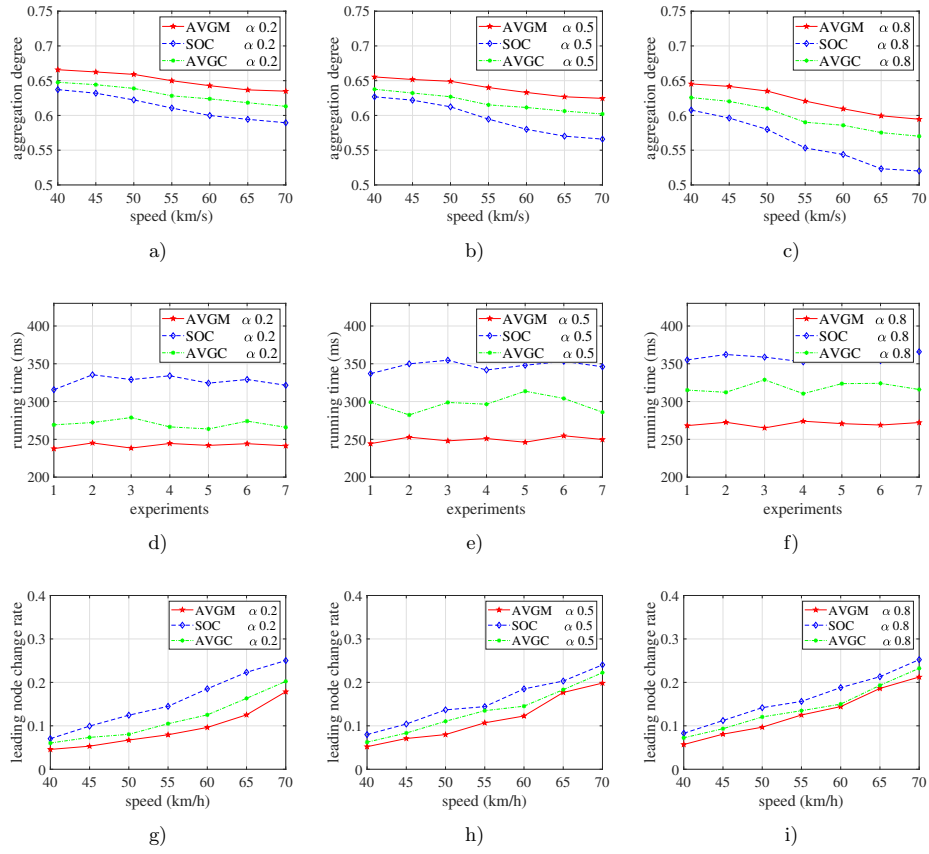

Figure 5. Simulation results of vehicle group models in a simulated closing scene. a)–c) compare the effect of changing speed on aggregation degree with different α values; d)–f) compare the running time of each algorithm with different α values, and g)–i) compare the effect of changing speed on the leading node change ratio with different α values.

as vehicle speed or α increases. This is because the mobility difference increases with them. AVGM's aggregation degree is higher than SOC's and AVGC's at different vehicle speed and α values, which verifies the effectiveness of our method.

The running time of AVGM, SOC, and AVGC at different experiments is shown in Figure 8. Experimental results show that AVGM's running time is shorter than SOC's and AVGC's. The running time of three methods increases with α values. This is because the vehicle group size increases with α values, which increases the time complexity of cooperation methods.

The relationship between leading node change rate and vehicle speed of AVGM, SOC, and AVGC with different α values is shown in Figure 9. AVGM's leading

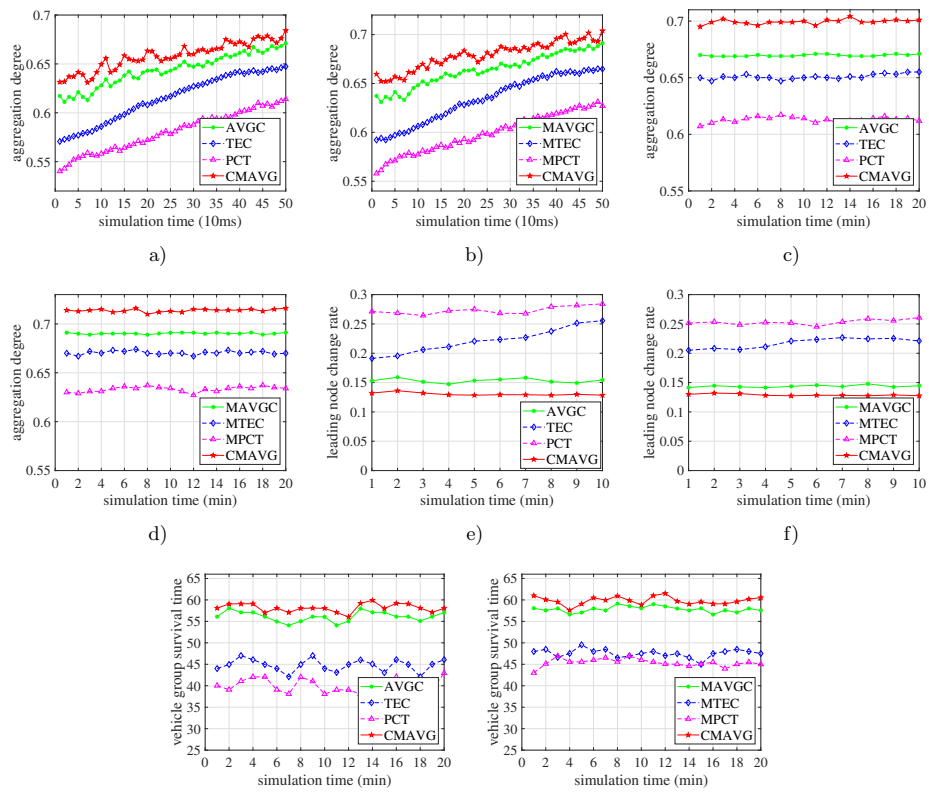

Figure 6. Simulation results of cooperative model in a simulated closing scene. a)–d) show the changing process of aggregation degree for a small time scale; c)–d) show the changing process of aggregation degree in the entire simulated process; e)–f) show the changing process of leading node change ratio; and g)–h) show the changing process of vehicle group survival time.

node change rate is lower than SOC's and AVGC's, which verifies the effectiveness of our method. The leading node change rate of three methods increases with vehicle speed because the speed difference between a leading node and vehicle group members increases with vehicle speed.

5.3.2 Performance of Cooperative Model in a Real Closing Scene

As shown in Figure 10, we show the aggregation degree of CMAVG, AVGC, TEC, and PCT in the first 0.5 s and the entire simulated process. CMAVG's aggregation degree is higher than AVGC's, TEC's, and PCT's, which verifies the effectiveness of our method. After using a multi-objective optimization method, AVGC's aggrega-

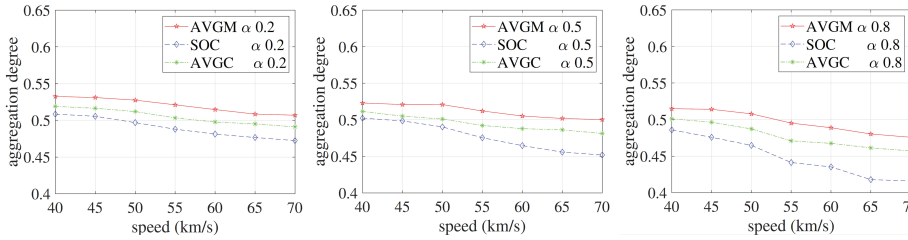

a) $\alpha = 0.2$ b) $\alpha = 0.5$ c) $\alpha = 0.8$

Figure 7. The effect of vehicle speed on aggregation degree with different α values

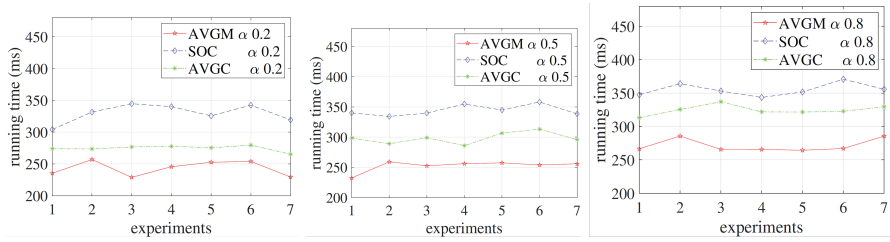

a) $\alpha = 0.2$ b) $\alpha = 0.5$ c) $\alpha = 0.8$

Figure 8. The running time of AVGM, SOC, and AVGC with different α values.

tion degree is improved by 5 %, which verifies the effectiveness of our multi-objective optimization method.

As shown in Figure 11, we show the leading node changing rate of CMAVG, AVGC, TEC, and PCT. CMAVG's leading node changing rate is lower than AVGC's, TEC's, and PCT's. This is because CMAVG considers association relationship among vehicle group members.

As shown in Figure 12, we show the vehicle group survival time of CMAVG, TEC, PCT, and AVGC with a period of 20 minutes. CMAVG outperforms the other three methods, which verifies the effectiveness of our method.

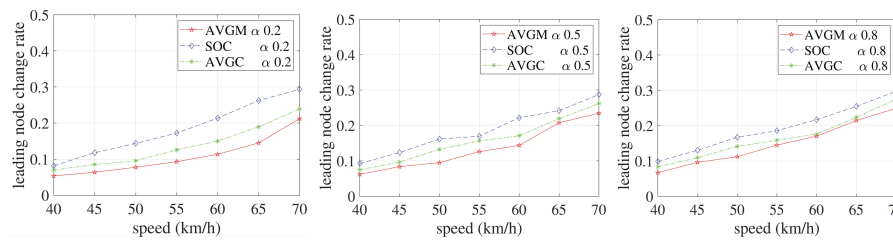

a) $\alpha = 0.2$ b) $\alpha = 0.5$ c) $\alpha = 0.8$

Figure 9. The effect of vehicle speed on leading node change ratio with different α values

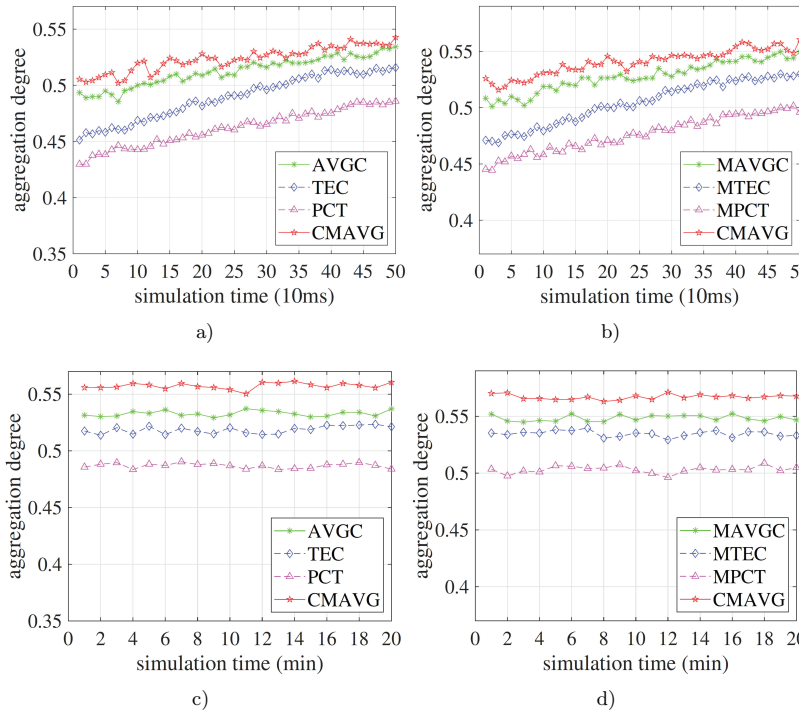

Figure 10. The aggregation degree of four cooperation methods

6 CONCLUSION

In this work, we construct an autonomous vehicle group model based on aggregation degree, formulate four events for autonomous vehicle groups, propose a cooperative model based on a state transition, and optimize a simulated annealing algorithm to solve the proposed cooperative model. Simulation results show that our formation method and cooperative method of autonomous vehicle groups outperform the existing five methods. Although our method shows good performance in vehicle group formation and cooperative behavior, we do not study applications of our models, which are areas of our future work. In addition, we will study wireless communication security and privacy protection of vehicle group members in future work.

Acknowledgements

This work was supported in part by the NSFC under Grant No. 62272344, and in part by the Natural Science Foundation of Shandong Province of China under Grant No. ZR2024QF107.

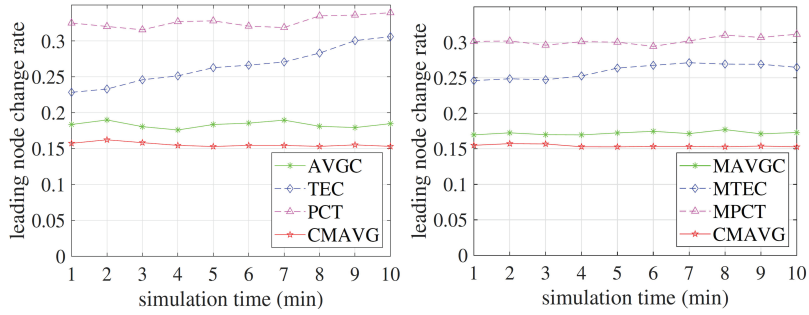

Figure 11. The changing process of leading node ratio of four cooperation methods

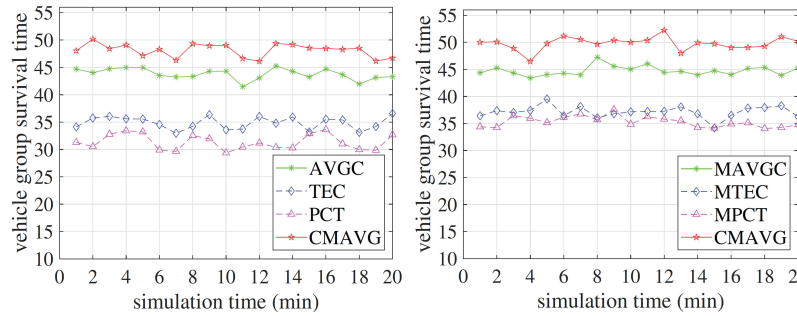

Figure 12. The changing process of vehicle group survival time of four cooperation methods

REFERENCES

[1] Milanés, V.—González, C.—Naranjo, J. E.—Onieva, E.—De Pedro, T.: Electro-Hydraulic Braking System for Autonomous Vehicles. International Journal of Automotive Technology, Vol. 11, 2010, No. 1, pp. 89–95, doi: 10.1007/s12239-010-0012-6.

[2] Anderson, J. M.—Nidhi, K.—Stanley, K. D.—Sorensen, P.—Samaras, C.—Oluwatola, O. A.: Autonomous Vehicle Technology: A Guide for Policymakers. RAND Corporation, 2014.

[3] Cheng, J.—Yuan, G.—Zhou, M.—Gao, S.—Huang, Z.—Liu, C.: A Connectivity-Prediction-Based Dynamic Clustering Model for VANET in an Urban Scene. IEEE Internet of Things Journal, Vol. 7, 2020, No. 9, pp. 8410–8418, doi: 10.1109/JIOT.2020.2990935.

[4] Cheng, J.—Yuan, G.—Zhou, M.—Gao, S.—Liu, C.—Duan, H.—Zeng, Q.: Accessibility Analysis and Modeling for IoV in an Urban Scene. IEEE Trans-

actions on Vehicular Technology, Vol. 69, 2020, No. 4, pp. 4246–4256, doi: 10.1109/TVT.2020.2970553.

[5] Zhang, J.—Cui, J.—Zhong, H.—Chen, Z.—Liu, L.: PA-CRT: Chinese Remainder Theorem Based Conditional Privacy-Preserving Authentication Scheme in Vehicular Ad-Hoc Networks. IEEE Transactions on Dependable and Secure Computing, 2021, No. 2, pp. 722–735, doi: 10.1109/TDSC.2019.2904274.

[6] Cui, J.—Zhang, X.—Zhong, H.—Zhang, J.—Liu, L.: Extensible Conditional Privacy Protection Authentication Scheme for Secure Vehicular Networks in a Multi-Cloud Environment. IEEE Transactions on Information Forensics and Security, Vol. 15, 2019, pp. 1654–1667, doi: 10.1109/TIFS.2019.2946933.

[7] Chen, C.—Xiao, T.—Qiu, T.—Lv, N.—Pei, Q.: Smart-Contract-Based Economical Platooning in Blockchain-Enabled Urban Internet of Vehicles. IEEE Transactions on Industrial Informatics, Vol. 16, 2020, No. 6, pp. 4122–4133, doi: 10.1109/TII.2019.2954213.

[8] Chen, C.—Hu, J.—Qiu, T.—Atiquzzaman, M.—Ren, Z.: CVCG: Cooperative V2V-Aided Transmission Scheme Based on Coalitional Game for Popular Content Distribution in Vehicular Ad-Hoc Networks. IEEE Transactions on Mobile Computing, Vol. 18, 2019, No. 12, pp. 2811–2828, doi: 10.1109/TMC.2018.2883312.

[9] Jalil, K.—Xia, Y.—Zahid, M. N.—Manzoor, T.: A Speed Optimization Strategy for Smooth Merging of Connected and Automated Vehicles at T-Shape Roundabout. IEEE Access, Vol. 10, 2022, pp. 76953–76965, doi: 10.1109/ACCESS.2022.3192774.

[10] Bakibillah, A. S. M.—Kamal, M. A. S.—Tan, C. P.—Susilawati, S.—Hayakawa, T.—Imura, J.: Bi-Level Coordinated Merging of Connected and Automated Vehicles at Roundabouts. Sensors, Vol. 21, 2021, No. 19, Art. No. 6533, doi: 10.3390/s21196533.

[11] Chang, H.—Ning, N.: An Intelligent Multimode Clustering Mechanism Using Driving Pattern Recognition in Cognitive Internet of Vehicles. Sensors, Vol. 21, 2021, No. 22, Art. No. 7588, doi: 10.3390/s21227588.

[12] Wang, Y.—Nakamura, M.—Sakakibara, K.: Modeling an Autonomous Vehicle Group Control System as a Hybrid Automaton and Its Specification and Verification in Rewriting Logic. 2021 36th International Technical Conference on Circuits/Systems, Computers and Communications (ITC-CSCC), IEEE, 2021, pp. 1–4, doi: 10.1109/ITC-CSCC52171.2021.9501418.

[13] Ghiasi, A.—Li, X.—Ma, J.: A Mixed Traffic Speed Harmonization Model with Connected Autonomous Vehicles. Transportation Research Part C: Emerging Technologies, Vol. 104, 2019, pp. 210–233, doi: 10.1016/j.trc.2019.05.005.

[14] Yu, C.—Wang, X.—Xu, X.—Zhang, M.—Ge, H.—Ren, J.—Sun, L.—Chen, B.—Tan, G.: Distributed Multiagent Coordinated Learning for Autonomous Driving in Highways Based on Dynamic Coordination Graphs. IEEE Transactions on Intelligent Transportation Systems, Vol. 21, 2020, No. 2, pp. 735–748, doi: 10.1109/TITS.2019.2893683.

[15] Nakamura, M.—Sakakibara, K.: Formal Verification and Mathematical Optimization for Autonomous Vehicle Group Controllers. 2019 ACM/IEEE 22nd Interna-

tional Conference on Model Driven Engineering Languages and Systems Companion (MODELS-C), 2019, pp. 732–733, doi: 10.1109/MODELS-C.2019.00111.

[16] Maiti, S.—Winter, S.—Kulik, L.—Sarkar, S.: Ad-Hoc Platoon Formation and Dissolution Strategies for Multi-Lane Highways. Journal of Intelligent Transportation Systems, Vol. 27, 2023, No. 2, pp. 161–173, doi: 10.1080/15472450.2021.1993212.

[17] Dokur, O.—Olenscki, G.—Katkoori, S.: Platoon Formation Based on DSRC Basic Safety Messages. 2022 IEEE International Symposium on Smart Electronic Systems (iSES), 2022, pp. 700–705, doi: 10.1109/iSES54909.2022.00155.

[18] El Ganaoui-Mourlan, O.—Camp, S.—Hannagan, T.—Arora, V.—De Neuville, M.—Kousournas, V. A.: Path Planning for Autonomous Platoon Formation. Sustainability, Vol. 13, 2021, No. 9, Art. No. 4668, doi: 10.3390/su13094668.

[19] Sreenivasamurthy, S.—Obraczka, K.: Towards Biologically Inspired Decentralized Platooning for Autonomous Vehicles. 2021 IEEE 93rd Vehicular Technology Conference (VTC2021-Spring), 2021, pp. 1–7, doi: 10.1109/VTC2021-Spring51267.2021.9448731.

[20] Wu, B.—Wu, Q.—Ying, Z.: [retracted] GAP-MM: 5G-Enabled Real-Time Autonomous Vehicle Platoon Membership Management Based on Blockchain. Security and Communication Networks, Vol. 2022, 2022, Art. No. 7567994, doi: 10.1155/2022/7567994.

[21] Xiong, X.—Sha, J.—Jin, L.: Optimizing Coordinated Vehicle Platooning: An Analytical Approach Based on Stochastic Dynamic Programming. Transportation Research Part B: Methodological, Vol. 150, 2021, pp. 482–502, doi: 10.1016/j.trb.2021.06.009.

[22] Ge, X.—Han, Q. L.—Wang, J.—Zhang, X. M.: Scalable and Resilient Platooning Control of Cooperative Automated Vehicles. IEEE Transactions on Vehicular Technology, Vol. 71, 2022, No. 4, pp. 3595–3608, doi: 10.1109/TVT.2022.3147371.

[23] Ye, Y. H.—Lin, Z. Y.—Yao, C. C.—Nguyen, L. H.—Kuo, J. J.—Hwang, R. H.: Efficient Multi-Maneuver Platooning Framework for Autonomous Vehicles on Multi-Lane Highways. 2021 IEEE 94th Vehicular Technology Conference (VTC2021-Fall), 2021, pp. 1–5, doi: 10.1109/VTC2021-Fall52928.2021.9625361.

[24] Kato, S.—Kunibe, M.—Yamazaki, R.—Shigeno, H.: Group Formation for Cooperative Highway Merging Considering Undetected Vehicles in Mixed Traffic. 2021 IEEE Vehicular Networking Conference (VNC), 2021, pp. 68–71, doi: 10.1109/VNC52810.2021.9644631.

[25] Zhou, J.—Zhu, F.: Analytical Analysis of the Effect of Maximum Platoon Size of Connected and Automated Vehicles. Transportation Research Part C: Emerging Technologies, Vol. 122, 2021, Art. No. 102882, doi: 10.1016/j.trc.2020.102882.

[26] Ledesma, S.—Aviña, G.—Sanchez, R.: Practical Considerations for Simulated Annealing Implementation. In: Tan, C. M. (Ed.): Simulated Annealing. IntechOpen, 2008, pp. 401–420.

[27] Hopcroft, J.—Khan, O.—Kulis, B.—Selman, B.: Tracking Evolving Communities in Large Linked Networks. Proceedings of the National Academy of Sciences (PNAS), Vol. 101, 2004, No. suppl_1, pp. 5249–5253, doi: 10.1073/pnas.0307750100.

[28] Haklay, M.—Weber, P.: OpenStreetMap: User-Generated Street Maps. IEEE Pervasive Computing, Vol. 7, 2008, No. 4, pp. 12–18, doi: 10.1109/MPRV.2008.80.

[29] Sutagundar, A. V.—Hubballi, P.—Belagali, R.: Stability Oriented Cluster Dynamism in VANET (SOCDV). 2016 International Conference on Computation System and Information Technology for Sustainable Solutions (CSITSS), 2016, pp. 117–120, doi: 10.1109/CSITSS.2016.7779406.

[30] Mao, Q.—Cheng, J.—Zhou, M.—Gao, S.—Han, S.: An Edge Computing-Based Autonomous Vehicle Group Cooperation Model in a Highway Scene. IEEE Transactions on Vehicular Technology, Vol. 73, 2024, No. 7, pp. 9682–9682, doi: 10.1109/TVT.2024.3375853.

[31] Kakkasageri, M. S.—Manvi, S. S.: Connectivity and Mobility Aware Dynamic Clustering in VANETs. International Journal of Future Computer and Communication, Vol. 3, 2014, No. 1, pp. 5–8, doi: 10.7763/IJFCC.2014.V3.256.

[32] Wang, S. S.—Lin, Y. S.: Performance Evaluation of Passive Clustering Based Techniques for Inter-Vehicle Communications. The 19th Annual Wireless and Optical Communications Conference (WOCC 2010), 2010, pp. 1–5, doi: 10.1109/WOCC.2010.5510657.

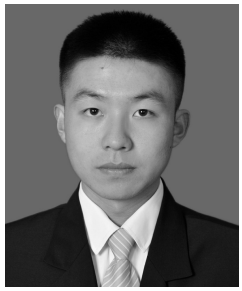

Guiyuan Yuan received his B.Sc. degree in computer science and technology and his M.Sc. degree in computer application technology from the Shandong University of Science and Technology, Qingdao, China, in 2015 and 2018, respectively, and his Ph.D. degree in computer science and technology from the Tongji University, Shanghai, China, in 2023. He is currently Lecturer of computer science and technology at the Shandong University of Science and Technology. He has authored over 20 technical papers in journals and conference proceedings. His research interests include Internet of Vehicles and autonomous cars.

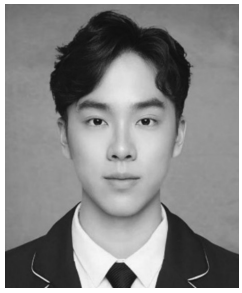

Jiake Wang is currently studying computer science and data science in the University of Sydney, Australia. His main research interests include autonomous driving, combat robot, and data computing based on 5G and edge-cloud.

Fengqi Yan received his M.Sc. degree in computer application technology from the Shandong University of Science and Technology, Qingdao, China, in 2007, and his Ph.D. degree in electronics and information from the Tongji University, Shanghai, China, in 2020. He is currently Professor at the School of Computer Science and Technology, Tongji University, Shanghai, China. His research interests include Big Data and artificial intelligence.

Feng Shen received his Ph.D. degree in traffic information engineering and control from the Tongji University, Shanghai, China in 2008. From 2008, he has been working at SEISYS, holding positions as the Chief Engineer of the company. He has over 16 years of experience in technical breakthroughs and product development in the fields of urban road traffic, public transportation, rail transit, and intelligent connected vehicles.

Xiangmei Li received her B.Sc. degree in computer software from the Shanghai Tiedao University and her M.Sc. degree in computer application from the Tongji University Shanghai, China, in 1993 and 2000. She is currently Associate Professor at the School of Computer Science and Technology, Tongji University, Shanghai, China. Her main research directions focus on multimedia technology and its applications.

Jiujun Cheng received his Ph.D. degree from the Beijing University of Posts and Telecommunications, in 2006. In 2009, he was a Visiting Professor with the Aalto University, Espoo, Finland. He is currently Professor with the Tongji University, Shanghai, China. He has over 100 publications including conference and journal articles. His current research interests include mobile computing, complex networks, Internet of Vehicles, and autonomous cars.